

A GUIDANCE FOR THE INTERPRETATION OF PROPAGATION SAW TESTS

Philipp L. Rosendahl^{1,*}, Valentin Adam^{1,2}, Stephan Harvey², Bastian Bergfeld², Florian Rheinschmidt¹, Melin D. E. Walet², Jakob Schöttner², Alec van Herwijnen², Philipp Weißgraeber³

¹Technical University of Darmstadt, Institute of Structural Mechanics and Design, Darmstadt, Germany

²WSL Institute for Snow and Avalanche Research SLF, Davos Dorf, Switzerland

³University of Rostock, Chair of Lightweight Design, Rostock, Germany

ABSTRACT: Assessing snowpack stability is crucial for determining the avalanche danger level. In this context, the propagation saw test is a valuable tool, though its results can be difficult to interpret. This paper aims to provide practical guidance for interpreting PST results by establishing direct connections between test outcomes and interpretable parameters. Despite nearly two decades of use, a definitive guide for PST interpretation is still lacking, with outcomes categorized as no propagation, crack arrest, or full propagation. We address the influence of factors such as slope angle and slab geometry on critical cut length and introduce an analytical model for real-time assessment. Utilizing data from 271 PSTs, we offer an interpretation tool to enhance comparability across different terrains and conditions.

Keywords: Dry-snow slab avalanches, fracture toughness, stability test, propagation saw test, propagation probability, real-time application

1. INTRODUCTION

Assessing snowpack stability is one of the most complex and challenging tasks in avalanche hazard management. Various stability tests, including the propagation saw test (PST), are routinely used in the field. Among these tests, the PST notably presents significant complexities in interpretation. Although it has been established almost two decades ago (van Herwijnen and Jamieson, 2005; Gauthier and Jamieson, 2008), conflicting interpretations persist, and a definitive user manual for assessing the results is still lacking.

A PST can result in three distinct scenarios: no propagation, crack arrest (with or without slab fracture), or full propagation. Interpreting the test results for any propagation scenario presents a key challenge: the inability to directly infer propagation probability from the measured critical cut length. This is because the critical cut length is heavily influenced by a long list of factors. Among others, these factors are

- slope angle
- cutting direction (upslope or downslope)
- slab end geometry (slope-normal or vertical)
- slab stiffness and strength
- stratification
- weak-layer stiffness and fracture toughness
- length-to-height ratio

Because the list is so long, the critical cut length alone does not allow for a comparison between different experimental conditions. Prominent examples are the effect of upslope or downslope cutting

(Bair et al., 2014; Adam et al., 2023), the differences when the slab ends are cut vertically or normal to the slope (Bergfeld et al., 2024), or the effect of inclination (Adam et al., 2024a).

However, the above studies have shown that, fundamentally, propagation is determined by the competition of the energy available for crack propagation on the crack driving side and the fracture toughness of the weak-layer on the material resistance side. To achieve comparability across different PSTs, we (1) calculate the weak-layer fracture toughness using a closed-form analytical model, effectively eliminating the influence of slab properties and geometric variations (Rosendahl and Weißgraeber, 2024). Next, (2) we analyze a comprehensive dataset of 271 full-propagation PSTs to derive the probability distribution of weak-layer fracture toughnesses, providing a quantitative measure of the relative weakness of the tested layers. The result is a metric that quantifies the likelihood of crack propagation in a snowpack.

Since no propagation and crack arrest are relatively straightforward indicators of limited crack extension potential, we focus our analysis on full propagation and provide an interpretation of the effective weakness of a snowpack that exhibits full propagation.

By offering an interpretation tool for the PST, we aim at enabling the immediate assessment of PST outcomes and at facilitating comparability between different geographical locations, terrain features, snowpacks conditions, etc., enhancing the transferability of these stability tests to potential hazards.

2. METHODS

Based on a closed-form analytical representation of stratified snowpacks (Rosendahl and Weißgrae-

*Corresponding author: rosendahl@ismd.tu-darmstadt.de

ber, 2020a,b; Weißgraeber and Rosendahl, 2023), we evaluate 271 full-propagation PSTs (van Herwijnen et al., 2016; Adam et al., 2024a) to develop a metric for the weakness of a snowpack with respect to crack propagation. Model and metric are implemented in a web application that allows for a readily interpretable, real-time evaluation of propagation saw tests.

2.1 Calculation of fracture toughnesses

We calculate weak-layer fracture toughnesses from PST results using the closed-form analytical model for the mechanical response of stratified snowpacks of Weißgraeber and Rosendahl (2023). The model requires PST geometry, slab properties, and critical cut length as inputs and provides the energy release rate, i.e., the energy available for crack expansion, as an output.

In a PST, the weak-layer crack will propagate when the energy release rate equals the fracture toughness of the weak layer

$$\mathcal{G}(a_c) = \mathcal{G}_c. \quad (1)$$

That is, the energy release rate at the critical cut length a_c is the fracture toughness of the weak layer.

To allow for the comprehensive evaluation of all PSTs in our dataset, we have extended the model by adding surface loads. The addition of surface loads was necessary in some experiments to produce specific and very diverse loading conditions (Adam et al., 2024a).

2.2 Dataset

We have evaluated cut lengths and stratigraphies from 271 full-propagation PSTs capturing inclinations from 0° to 65° , vertical and slope-normal slab faces, slab thicknesses between 10 cm and 177 cm, column lengths between 75 cm and 3 m, and mean slab densities between 170 kg/m^3 and 400 kg/m^3 (van Herwijnen et al., 2016; Adam et al., 2024a). From this dataset, we were able to determine the critical energy release rate from the measured critical cut length in the field. While the PSTs in the dataset were dominated by compressive loading, they comprise crack propagation under both pure shear and pure compression loading.

2.3 Distribution of fracture toughnesses

To identify the best-fit distribution function for the fracture toughness values within our dataset, we have tested the dataset (Fig. 1a) against several common probability distributions. The log-normal distribution with the probability density function

$$f(\mathcal{G}_c) = \frac{1}{\sqrt{2\pi}(\mathcal{G}_c - \theta)\sigma} \exp\left(-\frac{\ln^2\left(\frac{\mathcal{G}_c - \theta}{m}\right)}{2\sigma^2}\right), \quad (2)$$

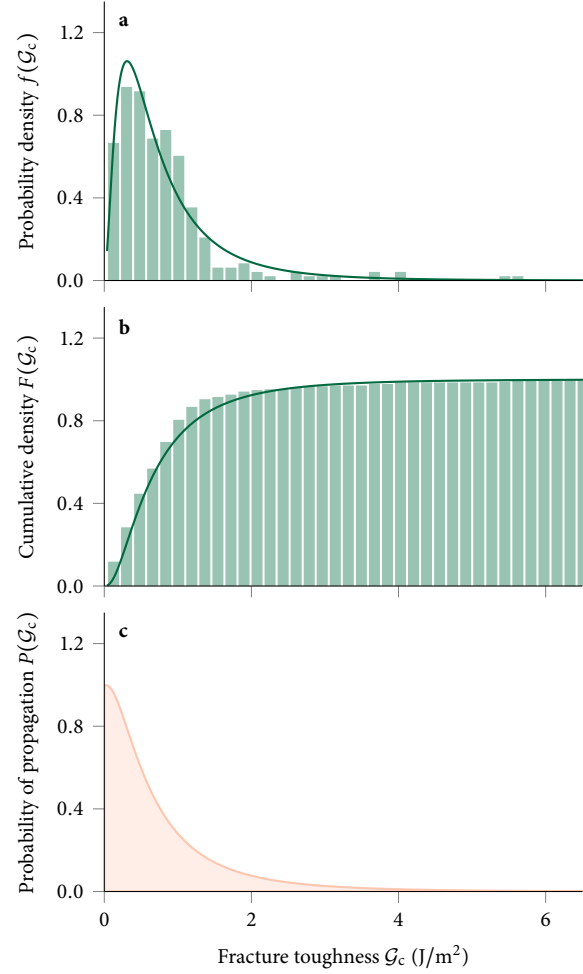


Figure 1: Frequency of weak-layer fracture toughness values. **a** Probability density of fracture toughnesses in our dataset ($N = 271$) with fitted log-normal probability density function, Eq. (2). **b** Cumulative probability of fracture toughnesses with the cumulative distribution function of the fitted log-normal distribution, Eq. (3). **c** Probability of crack propagation for fracture toughnesses measured in PSTs.

with shape, scale, and location parameters $\sigma = 0.80$, $m = 0.65$, and $\theta = -0.03 \text{ J/m}^2$, respectively, provided the best fit. The corresponding cumulative distribution function (Fig. 1b) is

$$F(\mathcal{G}_c) = \frac{1}{2} \left[1 + \operatorname{erf} \left(\frac{\ln\left(\frac{\mathcal{G}_c - \theta}{m}\right)}{\sqrt{2}\sigma} \right) \right], \quad (3)$$

where

$$\operatorname{erf}(x) = \frac{2}{\sqrt{\pi}} \int_0^x e^{-t^2} dt. \quad (4)$$

2.4 Probability of propagation

The probability P that a randomly chosen fracture toughness, X , from the population will be greater than or equal to a fracture-toughness measurement in a PST, x , is given by

$$P(X \geq x) = 1 - F(x). \quad (5)$$

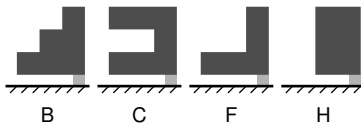


Figure 2: Illustration of benchmark snow profiles used in the present work. Material properties of hard, medium, and soft slab layers (dark) and the weak layer (light) are given in Table 1. The weak layer is 2 cm thick and the slab layers have a thickness of 12 cm each.

Table 1: Considered snow layers and their elastic properties with reference to three-layer slabs.

Layer	Hand hardness index	Density ρ (kg/m ³)	Young's modulus E (MPa)	Poisson's ratio ν
Hard	P	350	93.8	0.25
Medium	1F	270	30.0	0.25
Soft	4F	180	5.0	0.25
Weak layer	F-	100	0.15	0.25

This expresses the likelihood of finding a stronger weak layer in any PST. If we are likely to find a stronger weak-layer in another PST (P is high, \mathcal{G}_c is low, Fig. 1c), our snowpack is weak and large-scale crack propagation likely. If we are unlikely to find a stronger weak-layer in a different PST (P is low, \mathcal{G}_c is high, Fig. 1c), our snowpack is strong and large-scale crack propagation is less likely. Hence, P is a measure for the probability of crack propagation and serves as our standard of comparison.

This methodology does not distinguish between weak-layer grain types but aggregates the information gathered on many grain types, terrain forms, and aspects.

3. RESULTS AND DISCUSSION

Basing the interpretation of propagation saw tests on the energy release rate allows for comparison of seemingly similar, yet mechanically very different, scenarios. Compare upslope and downslope cuts of a PST of 1 m length with profile B (Fig. 2) on a 38° slope. Here, a critical upslope cut length of $a_c^\uparrow = 22.5$ cm yields a 50 % probability of propagation according to Eq. (5). Cutting the same PST from above (downslope) would need a result of $a_c^\downarrow = 42.7$ cm for a 50 % probability of propagation.

Similarly, the stratification of the snow cover has a significant effect on the likelihood of large-scale propagation. While a 45° downslope PST with a cut length $a_c^\downarrow = 20$ cm has a probability of 65 % with profile F (Fig. 2), it has a 45 % probability with profile C (Fig. 2). At the same cut length, the energy release rate under profile C is smaller than under profile F because C has a significantly higher bending stiffness. This is reflected in the smaller probability of C.

A homogeneous slab H (Fig. 2) has only a 2 % probability of finding a stronger weak layer at a cut length of $a_c = 50$ cm in flat terrain but a 42 % probability with an upslope cut at 45°.

4. CONCLUSIONS AND FUTURE WORK

We have shown that propagation saw tests can be unified and compared using the energy release rate of weak-layer cracks. For this purpose we have

- developed a closed-form analytical model for the assessment of PSTs,
- evaluated 271 full-propagation PSTs,
- identified a cumulative distribution function of weak-layer fracture toughnesses as a reference to compare full-propagation PST results,
- and implemented an easy-to-use web app.

While the current study focused only on full-propagation PSTs, the methodology can be extended to other PST outcomes. In future work, we will

- add additional full-propagation PSTs to refine the probability distribution of expected fracture toughnesses,
- identify a probability distribution for fracture toughnesses of crack-arrest PSTs to calculate and compare likelihoods for large-scale propagation and crack arrest,
- and incorporate slab properties and stresses to evaluate slab fracture.

ACKNOWLEDGMENTS

This work was in part supported by grants from the Swiss National Science Foundation (200021_169424 and 200021L_201071) and funded by the Deutsche Forschungsgemeinschaft (DFG, German Research Foundation) under grant no. 460195514.

CODE AVAILABILITY

A Python implementation of the mechanical model is publicly available from the code repository <https://github.com/2phi/weac> (Rosendahl and Weißgraeber, 2024) or for direct installation from <https://pypi.org/project/weac> (last accessed August 14, 2024).

DATA AVAILABILITY

The dataset including data processing routines is available under Creative Commons Attribution 4.0 International license from <https://doi.org/10.5281/zenodo.11443644> (Adam et al., 2024b).

REFERENCES

- Adam, V., Bergfeld, B., Rheinschmidt, F., Walet, M. D. E., Schöttner, J., Weißgraeber, P., Van Herwijnen, A., and Rosendahl, P. L.: A field test for the mixed-mode fracture toughness of weak layers, in: International Snow Science Workshop Proceedings 2023, Bend, Oregon, pp. 1261 – 1266, URL <http://arc.lib.montana.edu/snow-science/item/3042>, 2023.
- Adam, V., Bergfeld, B., Weißgraeber, P., van Herwijnen, A., and Rosendahl, P. L.: Fracture toughness of mixed-mode anticracks in highly porous materials, *Nature Communications*, (preprint), 2024a.
- Adam, V., Bergfeld, B., Weißgraeber, P., van Herwijnen, A., and Rosendahl, P. L.: Fracture toughness of mixed-mode anticracks in highly porous materials dataset and data processing, doi:10.5281/zenodo.11443644, 2024b.
- Bair, E. H., Simenhois, R., van Herwijnen, A., and Birkeland, K.: The influence of edge effects on crack propagation in snow stability tests, *The Cryosphere*, 8, 1407–1418, doi:10.5194/tc-8-1407-2014, URL <https://tc.copernicus.org/articles/8/1407/2014/>, 2014.
- Bergfeld, B., Birkeland, K. W., Adam, V., Rosendahl, P. L., and van Herwijnen, A.: The effect of propagation saw test geometries on critical cut length, *EGUsphere*, (preprint), doi:10.5194/egusphere-2024-690, 2024.
- Gauthier, D. and Jamieson, B.: Fracture propagation propensity in relation to snow slab avalanche release: Validating the Propagation Saw Test, *Geophysical Research Letters*, 35, doi:10.1029/2008GL034245, 2008.
- Rosendahl, P. L. and Weißgraeber, P.: Modeling snow slab avalanches caused by weak-layer failure – Part 1: Slabs on compliant and collapsible weak layers, *The Cryosphere*, 14, 115–130, doi:10.5194/tc-14-115-2020, URL <https://www.the-cryosphere.net/14/115/2020/>, 2020a.
- Rosendahl, P. L. and Weißgraeber, P.: Modeling snow slab avalanches caused by weak-layer failure – Part 2: Coupled mixed-mode criterion for skier-triggered anticracks, *The Cryosphere*, 14, 131–145, doi:10.5194/tc-14-131-2020, URL <https://www.the-cryosphere.net/14/131/2020/>, 2020b.
- Rosendahl, P. L. and Weißgraeber, P.: Weak Layer Anticrack Nucleation Model (WEAC), doi:10.5281/zenodo.5810763, URL <https://github.com/2phi/weac>, 2024.
- van Herwijnen, A. and Jamieson, B.: High-speed photography of fractures in weak snowpack layers, *Cold Regions Science and Technology*, 43, 71–82, doi:10.1016/j.coldregions.2005.05.005, 2005.
- van Herwijnen, A., Gaume, J., Bair, E. H., Reuter, B., Birkeland, K. W., and Schweizer, J.: Estimating the effective elastic modulus and specific fracture energy of snowpack layers from field experiments, *Journal of Glaciology*, 62, 997–1007, doi:10.1017/jog.2016.90, 2016.
- Weißgraeber, P. and Rosendahl, P. L.: A closed-form model for layered snow slabs, *The Cryosphere*, 17, 1475–1496, doi:10.5194/tc-17-1475-2023, URL <https://tc.copernicus.org/articles/17/1475/2023/>, 2023.